

Electronic Supporting Information (ESI)

**CoS<sub>2</sub>-TiO<sub>2</sub> Hybrid Nanostructures: Efficient and Durable Oxygen  
Evolution Catalysts for the Alkaline Electrolyte Membrane Water  
Electrolyzers**

Pandian Ganesan, Arumugam Sivanantham and Sangaraju Shanmugam\*

Department of Energy Science & Engineering,  
Daegu Gyeongbuk Institute of Science & Technology (DGIST),  
50-1 Sang-Ri, Hyeonpung-Myeon, Dalseong-gun,  
Daegu, 42988, Republic of Korea.  
E-mail: [sangarajus@dgist.ac.kr](mailto:sangarajus@dgist.ac.kr); Tel: +82-53-785-6413.

## Calculation of lattice parameter

d-spacing calculated from Bragg's equation,

$$n\lambda = 2d\sin\theta$$

Where  $\lambda$ ,  $\theta$  and  $d$  are wave length of X-ray, angle of diffraction and  $d$  is the distance between the two consecutive planes.

In case of the cubic symmetry,

$$\frac{1}{d^2} = \frac{h^2 + k^2 + l^2}{a^2}$$

But, in case of the cubic symmetry,

$$\frac{1}{d^2} = \frac{h^2}{a'^2} + \frac{1}{c^2}$$

Where  $h$ ,  $k$  and  $l$  are lattice planes,  $a$ ,  $a'$  and  $b$  are lattice parameter in Å.

## Calculations of Thermal Gravimetric Analysis (TGA)

TGA of the pure  $\text{CoS}_2$  prepared from the cobalt thiourea complex exhibits 82% loss. Hence, 18% of  $\text{CoS}_2$  were not completely decomposed. Also, pure  $\text{TiO}_2$  exhibits the weight loss of 6.7%. Hence,

$$\text{Weight loss due to only } \text{CoS}_2 \text{ in each samples} = \frac{\text{Total weight loss of the composite}}{\text{TiO}_2 \text{ weight loss}} - \text{TiO}_2 \text{ weight loss}$$

$$\text{Then, remaining \% of } \text{CoS}_2 = \frac{18}{81} * \text{CoS}_2 \text{ weight loss in each composites}$$

$$\text{Hence, total \% of } \text{CoS}_2 = \text{Remaining \% of } \text{CoS}_2 + \text{Weight lost by } \text{CoS}_2 \text{ only}$$

## Band gap from the UV-visible spectroscopy

The band gap of the UV-visible spectra in the Figure 6 can be calculated by plotting the  $(\alpha h\nu)^2$  in the y-axis and band gap calculated  $E_g$  from the incident wavelength for each material.

Where  $\alpha$  is the absorption coefficient,  $h$  is Planck's constant,  $\nu$  is frequency of the wavelength.

$A$  is calculated using the relationship

$$A = \frac{2.303 * A}{t}$$

where  $A$  is absorbance,  $t$  is the thickness of the sample.

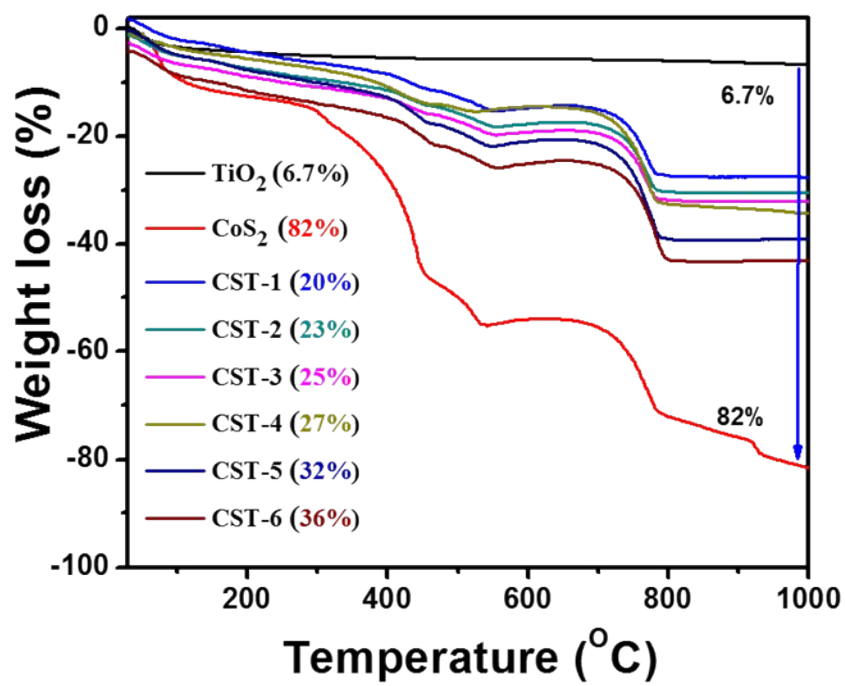
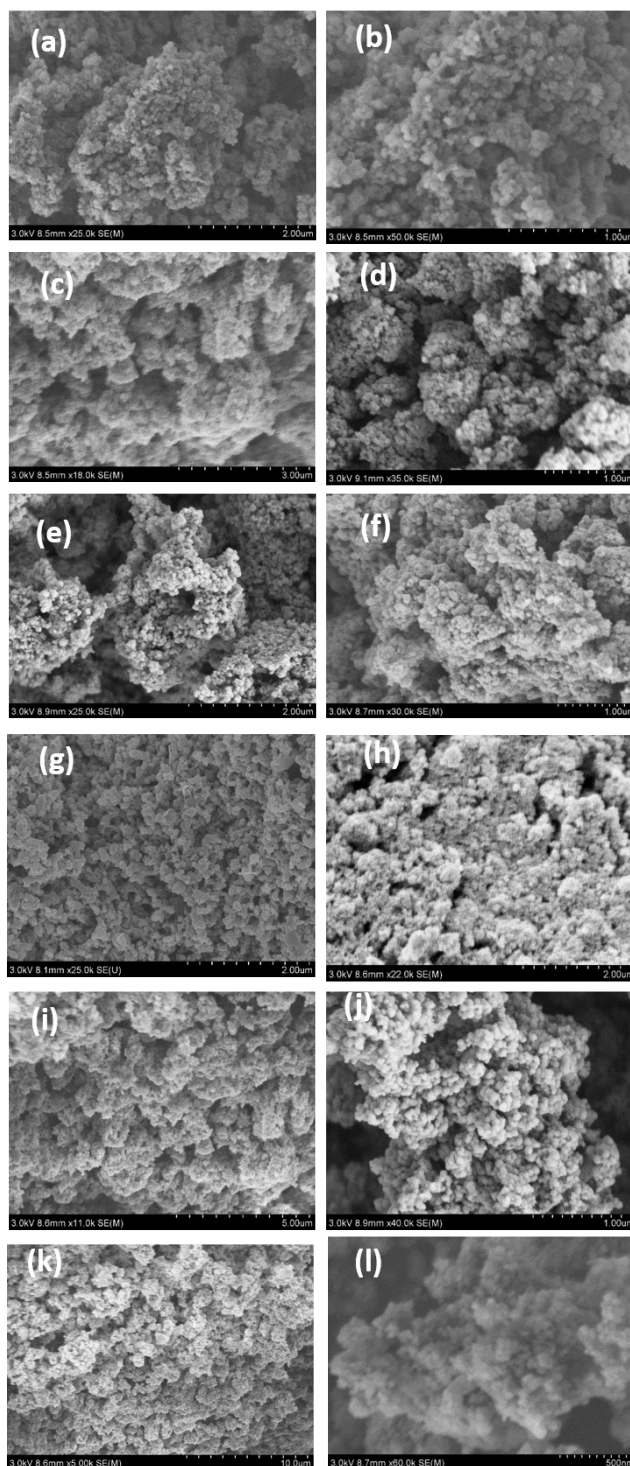
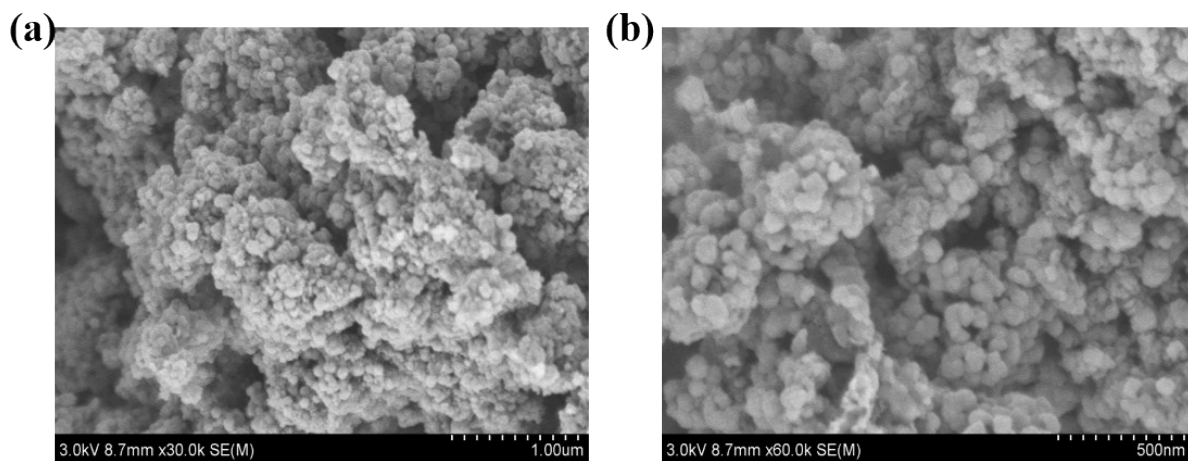


Fig. S1 TGA of CST-1, CST-2, CST-3, CST-4, CST-5, CST-6, CoS<sub>2</sub> and TiO<sub>2</sub>.



**Fig. S2** SEM images: low and high magnification images of CST-1 (a &b), CST-2 (c &d), CST-3 (e &f), CST-4 (g &h), CST-5 (i &j) and CST-6 (k &l).



**Fig S3:** (a) Low and (b) high magnification images of pristine TiO<sub>2</sub>.

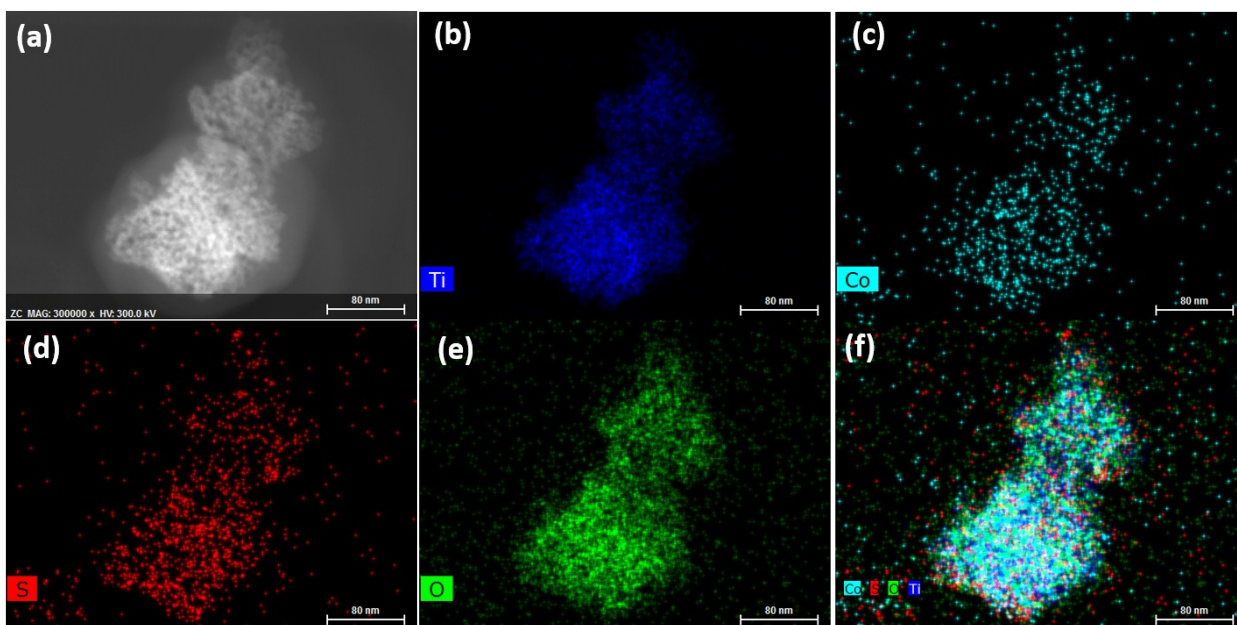


**Fig. S4** TEM elemental mapping analysis of CST-3 (a) Selected area and corresponding elemental mapping for (b) Titanium (c) Cobalt, (d) sulfur, (e) oxygen and (f) combined elements.

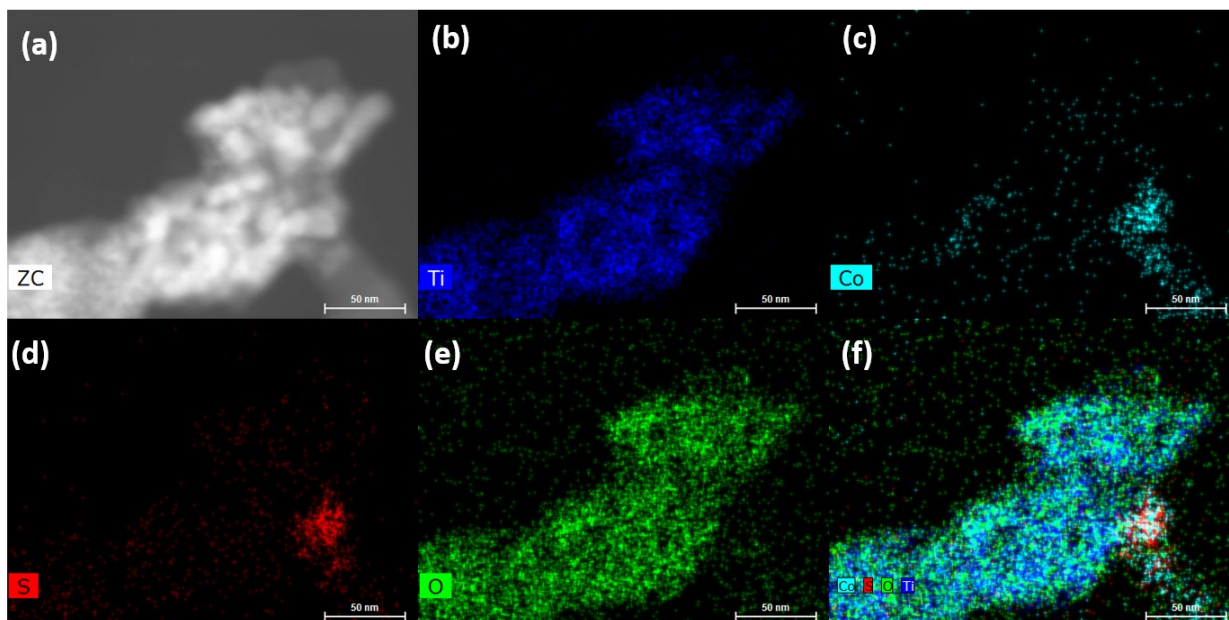


**Fig. S5** TEM elemental mapping analysis of CST-5 (a) Selected area and corresponding elemental mapping for (b) Titanium (c) Cobalt, (d) sulfur, (e) oxygen and (f) combined elements.

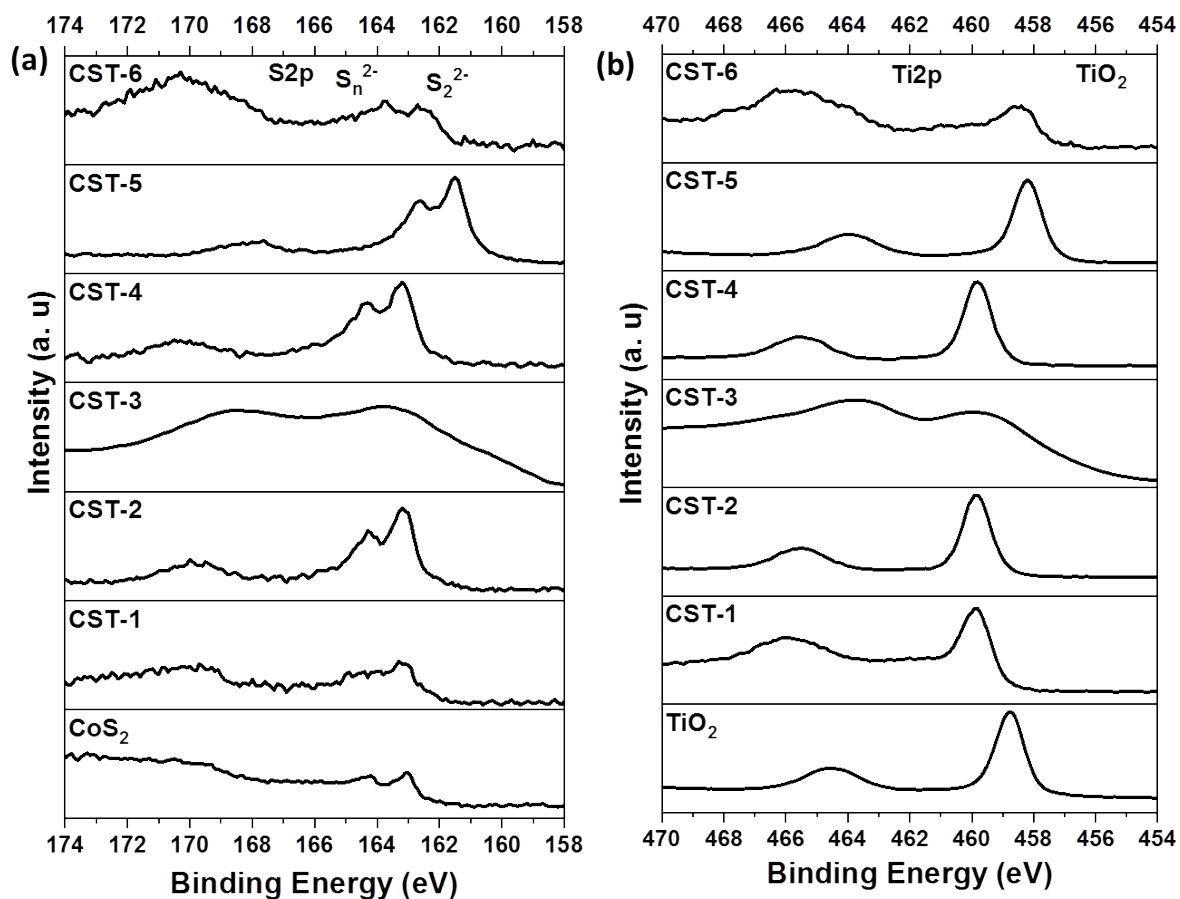


**Fig. S6** (a) The XPS spectra of CoS<sub>2</sub>, CST-1, CST-2, CST-3, CST-4, CST-5 and CST-6 in the S2p region. (b) The XPS spectra of TiO<sub>2</sub>, CST-1, CST-2, CST-3, CST-4, CST-5 and CST-6 in the Ti2p region.

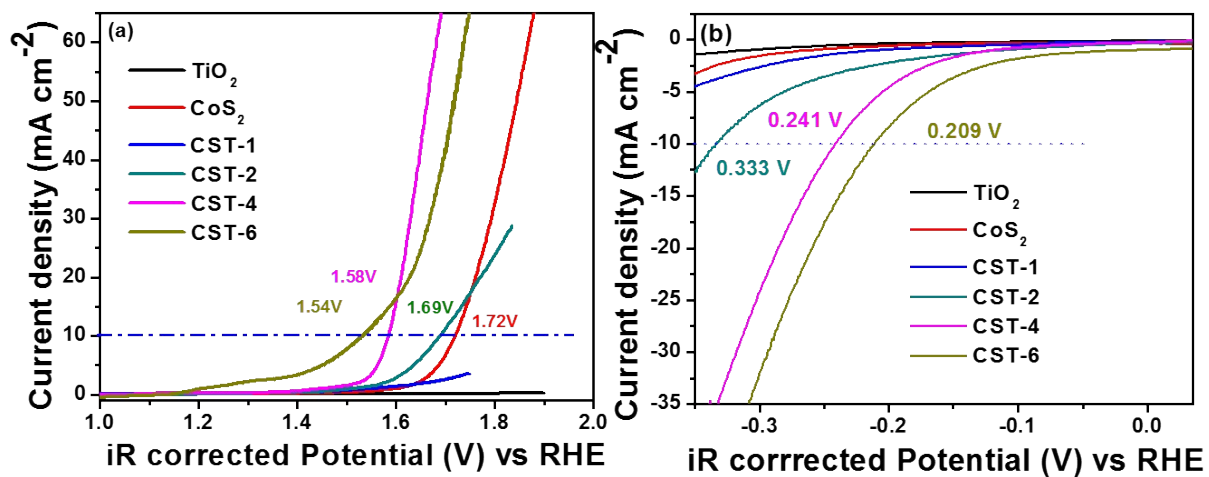


**Fig. S7** (a) The OER polarization curves of TiO<sub>2</sub>, CoS<sub>2</sub>, CST-1, CST-2, CST-4 and CST-6 and (b) and the HER polarization curves of TiO<sub>2</sub>, CoS<sub>2</sub>, CST-1, CST-2, CST-4 and CST-6 in 1 M KOH at the 10 mV s<sup>-1</sup> scan rate.

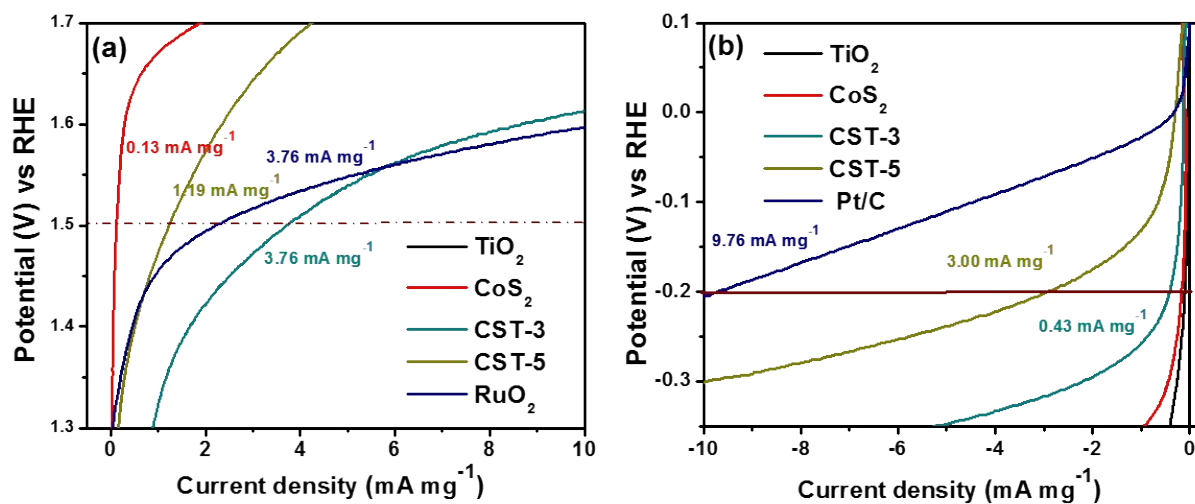


**Fig. S8** (a) The OER mass activities of  $\text{TiO}_2$ ,  $\text{CoS}_2$ , CST-3, CST-5 and  $\text{RuO}_2$ . (b) The HER mass activities of  $\text{TiO}_2$ ,  $\text{CoS}_2$ , CST-3, CST-5 and Pt/C.

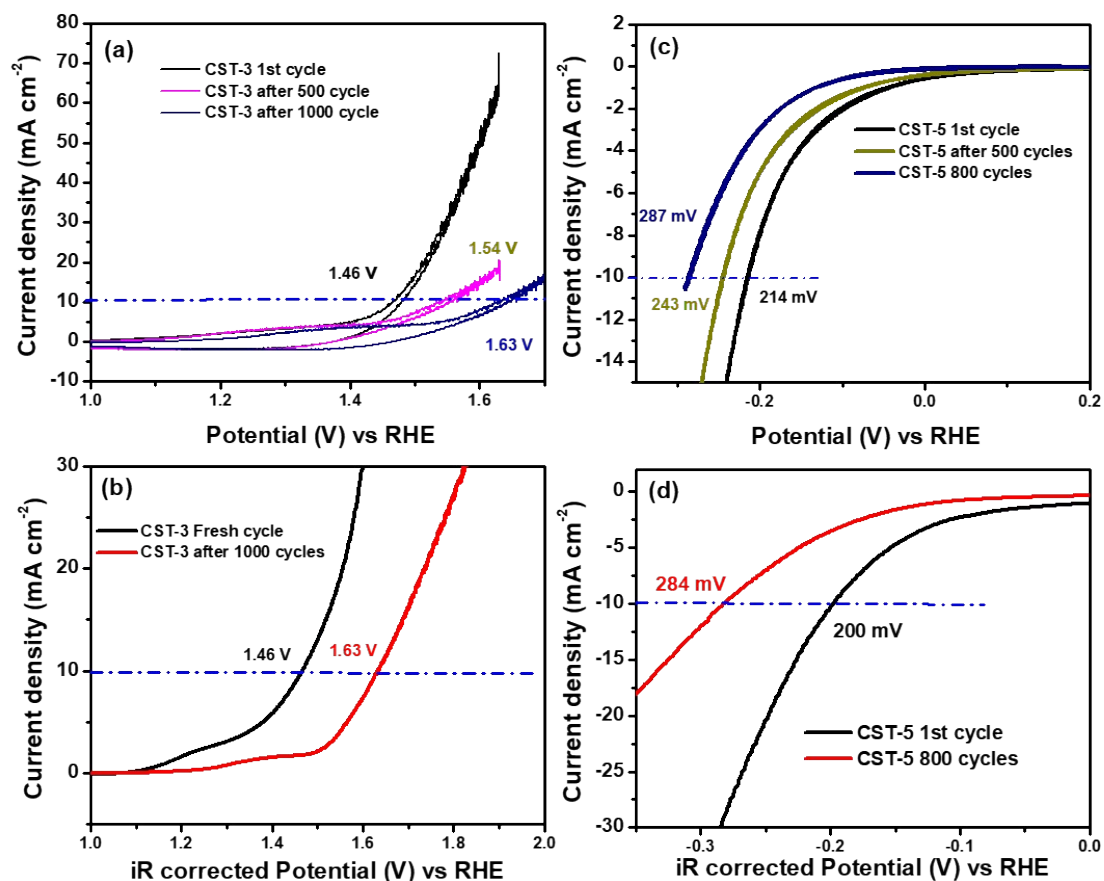


**Fig. S9** (a) The OER cyclic voltammetric (CV) stability test of CST-3 catalysts. (b) The corresponding OER linear sweep voltammetry of CST-3 before stability test and after 1000 cycles of the CV test. (c) The HER cyclic voltammetric (CV) stability test of CST-5 catalysts. (d) The corresponding HER linear sweep voltammetry of CST-5 before stability test and after 800 cycles of the CV test.

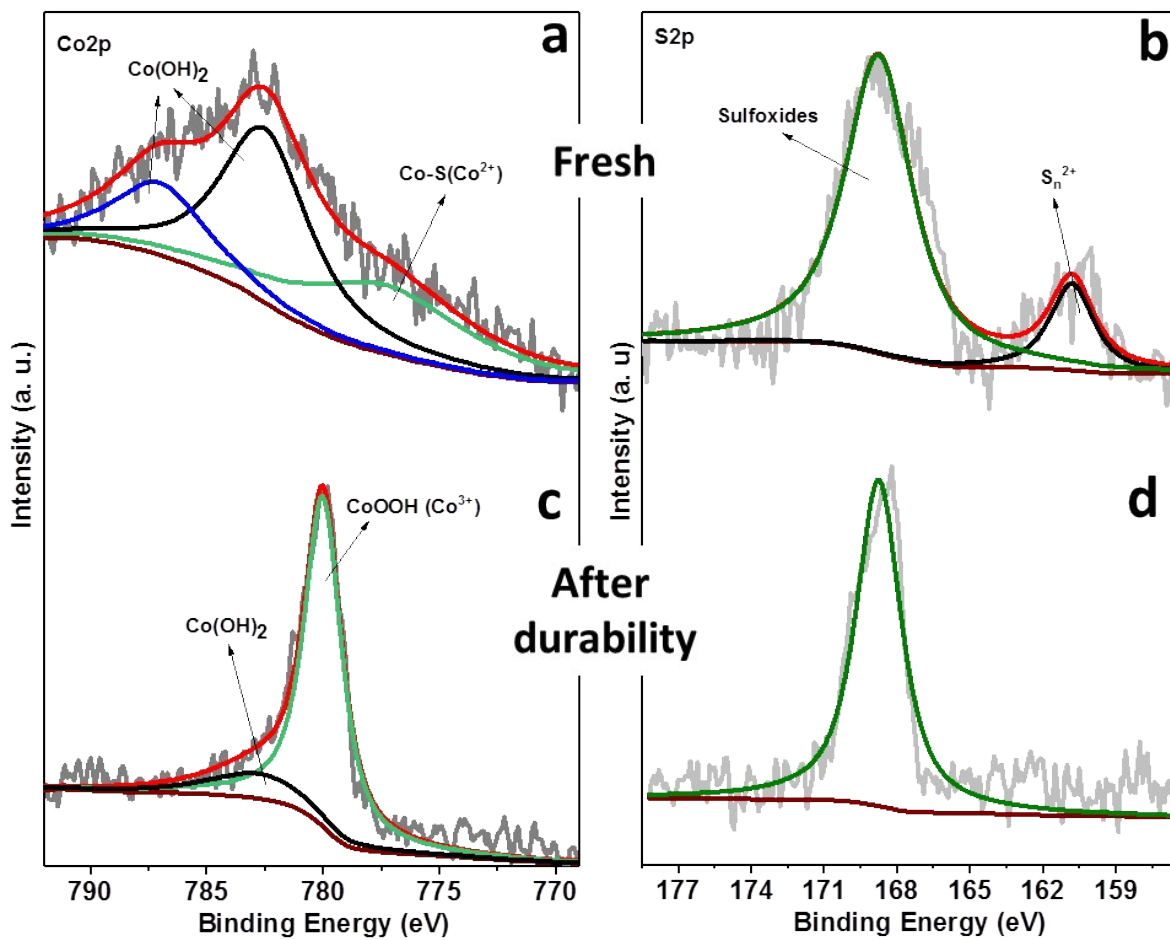


**Fig. S10** Post XPS analysis (Co2p and S2p) and comparison of CST-3 catalyst: (a,b) fresh catalyst and (c,d) after 1000 cycles of OER durability test.

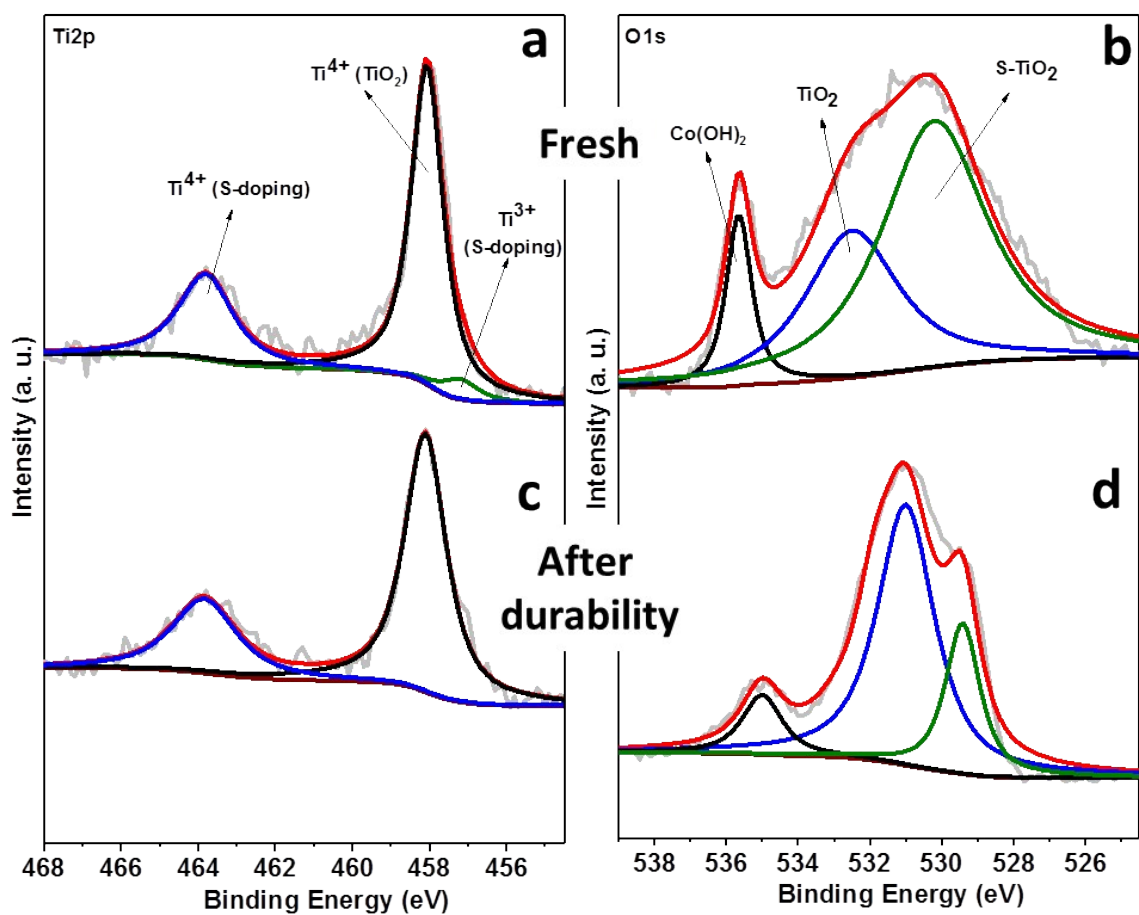


**Fig. S11** Post XPS analysis (Ti2p and O1s) and comparison of CST-3 catalyst: (a,b) fresh catalyst and (c,d) after 1000 cycles of OER durability test.

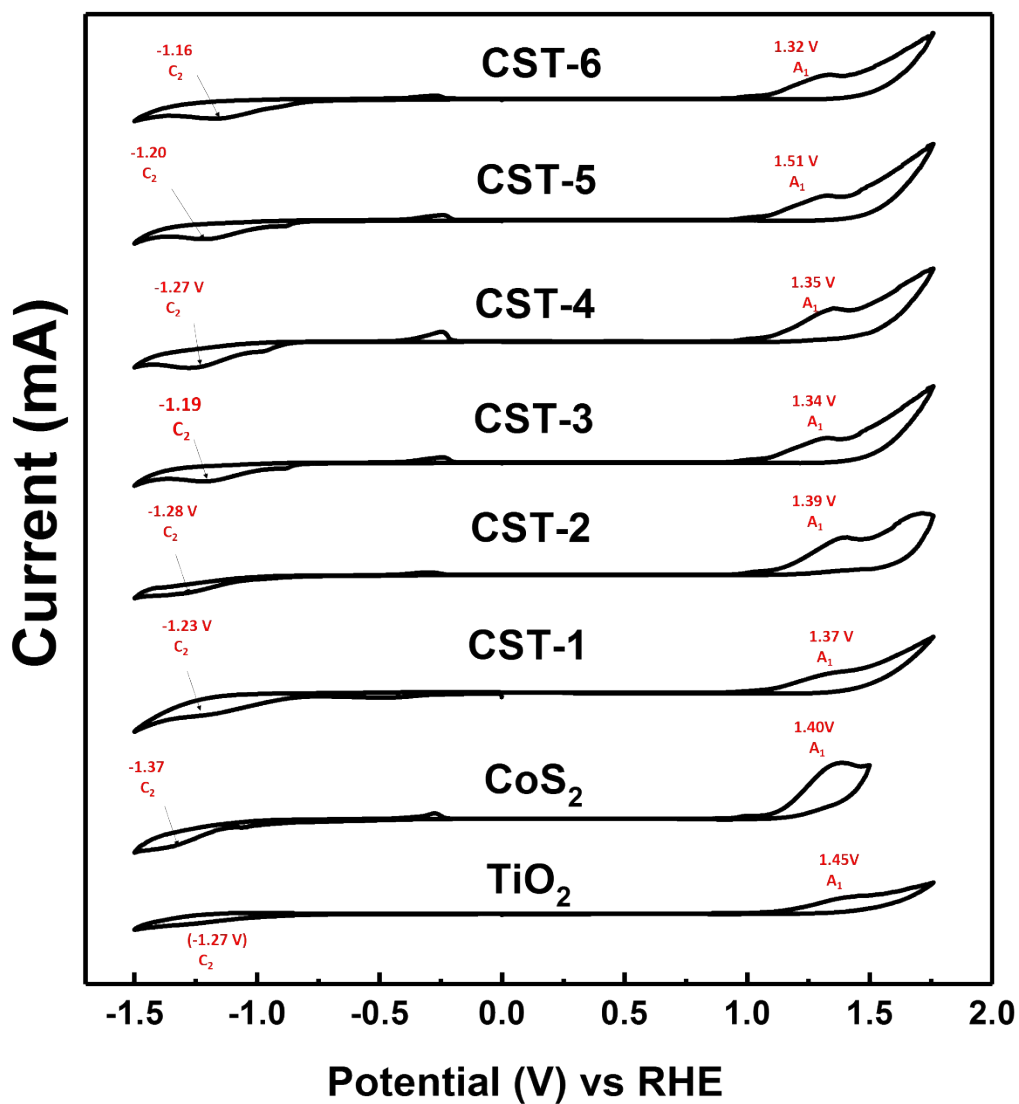


**Fig. S12** Electrochemical band gap of the TiO<sub>2</sub>, CST-1, CST-2, CST-3, CST-4, CST-5, CST-6 and CoS<sub>2</sub> electrodes.

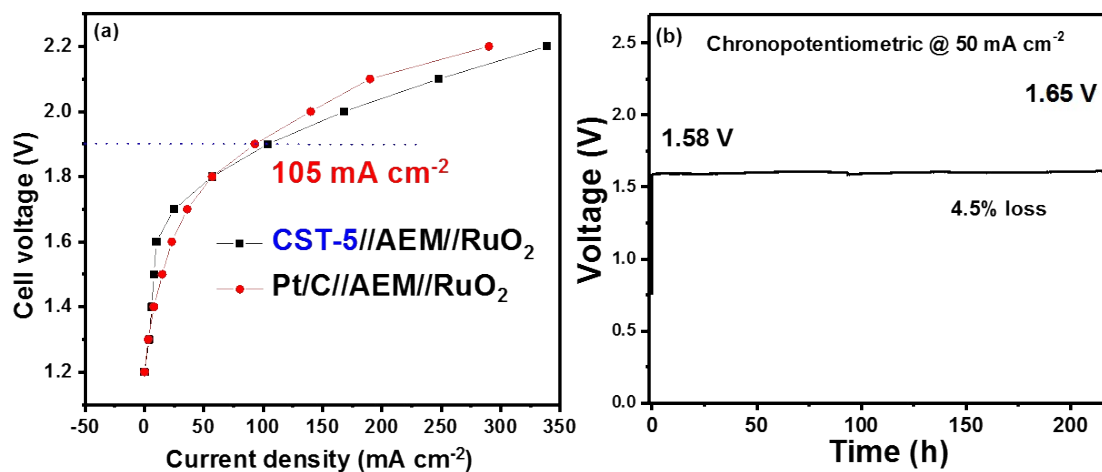


**Fig. S13** (a) The cell voltage versus current density of the AEM constructed with the CST-5//AEM//RuO<sub>2</sub> and Pt/C//AEM//RuO<sub>2</sub>. (b) The corresponding chronopotentiometric durability of CST-5//AEM//RuO<sub>2</sub> at 50 mA cm<sup>-2</sup>.

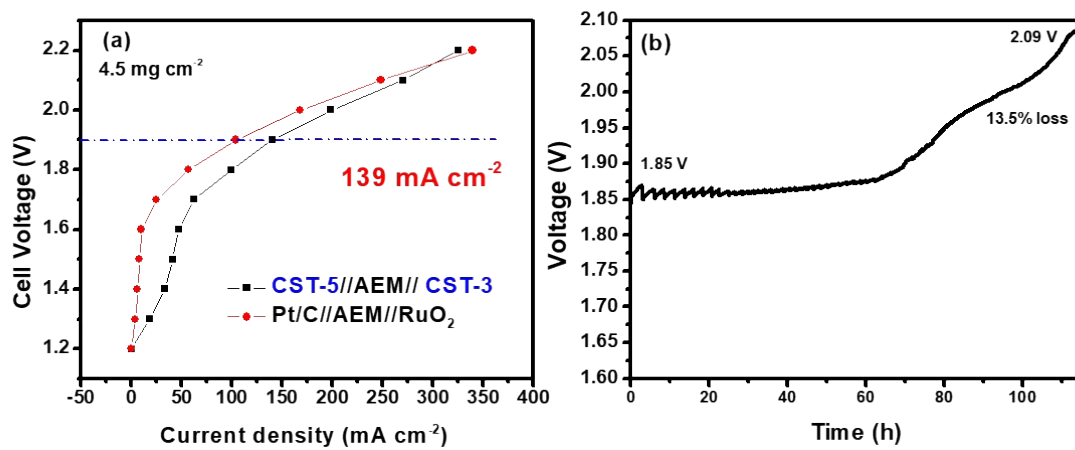


**Fig. S14.** (a) The cell voltage versus current density of the AEM constructed with the CST-5//AEM//CST-3. (b) The corresponding chronopotentiometric durability of CST-5//AEM//CST-3 at 100 mA cm<sup>-2</sup>.

### Calibration of Hg/HgO electrode to RHE (reversible hydrogen electrode).

We have calibrated the Hg/HgO electrode with respect to the reversible hydrogen electrode (RHE) at high purity hydrogen saturated 1 M KOH with the Pt wire as the working electrode. The cyclic voltammetry was carried out and the average of the two potentials (1.022 and 0.98 V) at which the current crossed zero was taken to be the thermodynamic potential (1.001 V) (Fig. S9).

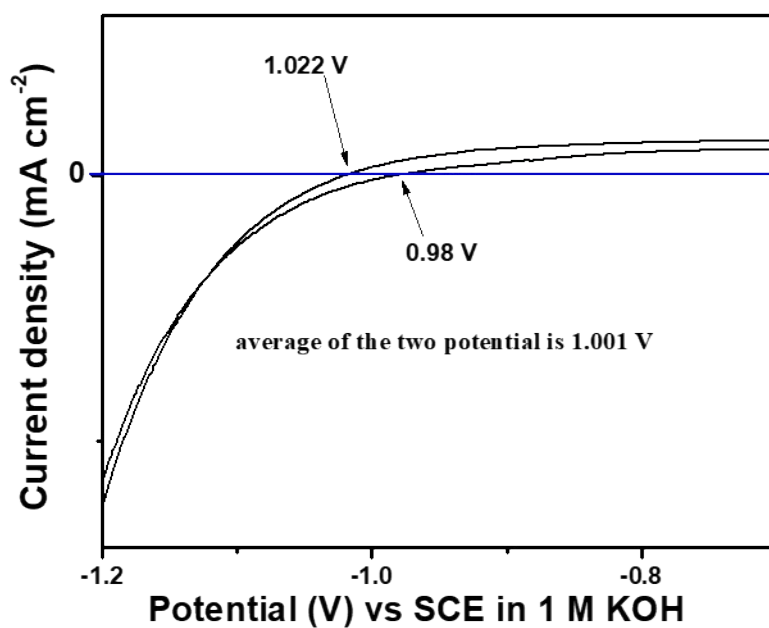


**Fig. S15** The calibration curve of the Hg/HgO electrode for the conversion of reversible hydrogen electrode (RHE).

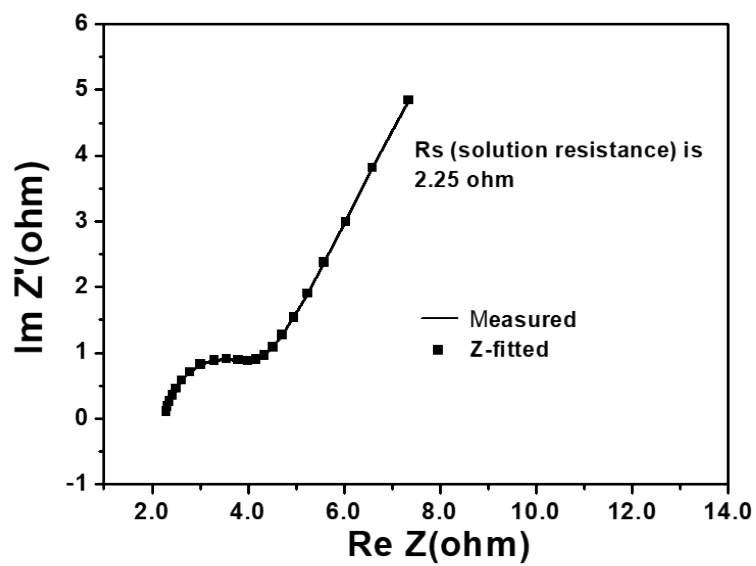


**Fig. S16** The electrochemical impedance spectra (EIS) in 1 M KOH using the glassy carbon electrode.

**Table S1.** The measured cell parameter from XRD pattern for various CoS<sub>2</sub>-TiO<sub>2</sub> hybrids and ratios of CoS<sub>2</sub> and TiO<sub>2</sub> from TGA.

Catalysts	Cell parameter CoS <sub>2</sub> (Cubic symmetry)	Cell parameter TiO <sub>2</sub> (Tetragonal symmetry)	
	a (Å)	a' (Å)	b(Å)
TiO <sub>2</sub>	-	3.7872	9.6140
CoS <sub>2</sub>	5.5530	-	-
CST-1	5.5502	3.8042	9.6140
CST-2	5.5436	3.8042	9.6140
CST-3	5.5430	3.8040	9.6140
CST-4	5.5412	3.8040	9.6140
CST-5	5.5404	3.8036	9.6140
CST-6	5.5376	3.8030	9.6140

**Table S2.** Calculation of CoS<sub>2</sub> and TiO<sub>2</sub> ratio using the TGA results.

Catalysts	Total weight loss of the composite (CoS <sub>2</sub> + TiO <sub>2</sub> ) (%)	Weight loss due to only CoS <sub>2</sub> (%)	Remaining % of CoS <sub>2</sub>	Total amount of CoS <sub>2</sub> (%)	Total amount of TiO <sub>2</sub> (%)
CST-1	27	20.3	6.4611	27	73
CST-2	30	23.3	7.179	31	69
CST-3	32	25.3	7.6576	33	67
CST-4	34	27.3	8.1362	35	65
CST-5	39	32.3	9.3327	42	58
CST-6	43	36.3	10.2899	47	53

**Table S3.** OER mass activities (MA) and turn over frequencies (TOF) of various catalysts.

Catalysts	OER	
	TOF @ 1.50 V $\times 10^{-3}$ (s <sup>-1</sup> )	Mass activity @ 1.50 V (mA mg <sup>-1</sup> )
CoS <sub>2</sub>	0.1	0.13
CST-3	5.2	3.76
CST-5	3.3	1.19
RuO <sub>2</sub>	1.2	2.76

**Table S4.** Comparison of OER activities with recent non-precious catalysts in 1 M KOH.

Catalysts	OER	References
	Overpotential $\eta$ (mV) @10 mA cm <sup>-2</sup>	
CST-3	231	This work
Ni <sub>3</sub> S <sub>2</sub> /NF	260	<i>J. Am. Chem. Soc.</i> , 2015, <b>137</b> , 14023.
CoSe/Ti mesh	341	<i>Chem. Commun.</i> , 2015, <b>51</b> , 16683.
Ni <sub>3</sub> Se <sub>2</sub> -Ni foam	270	<i>Energy Environ. Sci.</i> , 2016, <b>9</b> , 1771.
AgCuZn-S	361	<i>ACS Appl. Mater. Interfaces</i> , 2015, <b>7</b> , 17112.
CoTe <sub>2</sub> /CNT	239	<i>J. Phys. Chem. C</i> , 2016, <b>120</b> , 28093.
Co <sub>9</sub> S <sub>8</sub> microplates	278	<i>ACS Appl. Mater. Interfaces</i> , 2017, <b>9</b> , 11634.
ECT-CoO	346	<i>ACS Cent. Sci.</i> , 2015, <b>1</b> , 244.
Co <sub>9</sub> S <sub>8</sub> /CNS	394	<i>J. Mater. Chem. A</i> , 2016, <b>4</b> , 18314.
ECT-Se-Co <sub>0.5</sub> Fe <sub>0.5</sub> O	243	<i>Nano Lett.</i> , 2016, <b>16</b> , 7588.
Co@CoO/NG	315	<i>J. Mater. Chem. A</i> , 2016, <b>4</b> , 12046
Co <sub>1-x</sub> Fe <sub>x</sub> S@N-MC	410	<i>ACS Appl. Mater. Interfaces</i> , 2015, <b>7</b> , 1207.
Ni <sub><math>\alpha</math></sub> Co <sub>3-<math>\alpha</math></sub> O <sub>4</sub> nanowires	337	<i>ACS Appl. Mater. Interfaces</i> 2016, <b>8</b> , 3208.

**Table S5.** Comparison of HER activities with recent non-precious catalysts in 1 M KOH.

Catalysts	HER	References
	Overpotential $\eta$ (mV) @ -10 mA cm <sup>-2</sup>	
<b>CST-5</b>	<b>200</b>	<b>This work</b>
Ni <sub>3</sub> S <sub>2</sub> /NF	223	<i>J. Am. Chem. Soc.</i> , 2015, <b>137</b> , 14023.
MoS <sub>x</sub>	540	<i>Chem. Commun.</i> , 2015, <b>51</b> , 16683.
CoP/CC	209	<i>J. Am. Chem. Soc.</i> , 2014, <b>136</b> , 7587
$\beta$ -NiS NCs	250	<i>RSC Adv.</i> , 2015, <b>5</b> , 104740.
Ni-S/FTO	330	<i>J. Mater. Chem. A</i> , 2014, <b>2</b> , 19407.
Ni <sub>3</sub> S <sub>2</sub>	335	<i>Catal. Sci. Technol.</i> , 2016, <b>6</b> , 1077.
NiTe <sub>2</sub>	256	<i>Nanoscale</i> , 2017, <b>9</b> , 5538.
Co <sub>9</sub> S <sub>8</sub> @NPC-10	261	<i>RSC Adv.</i> , 2017, <b>7</b> , 19181.
Co <sub>x</sub> @CN	232	<i>J. Am. Chem. Soc.</i> , 2015, <b>137</b> , 2688.
Co-Ni-G	330	<i>RSC Adv.</i> , 2015, <b>5</b> , 47398.
Co embedded Nickel on carbon	249	<i>J. Mater. Chem. A</i> , 2016, <b>4</b> , 12818.

**Table S6.** The optical and electrochemical band gap values of various CoS<sub>2</sub>-TiO<sub>2</sub> hybrids.

Catalysts	Optical Band gap (E <sub>g</sub> ) eV	C <sub>1</sub> V vs. RHE	A <sub>1</sub> V vs. RHE	Electrochemical Band gap (E <sub>g</sub> ) eV
TiO <sub>2</sub>	3.08	-1.27	1.45	2.72
CST-1	2.85	-1.23	1.37	2.60
CST-2	2.80	-1.28	1.39	2.67
CST-3	2.60	-1.20	1.29	2.53
CST-4	2.44	-1.27	1.35	2.62
CST-5	2.52	-1.21	1.34	2.51
CST-6	2.91	-1.16	1.32	2.48
CoS <sub>2</sub>	2.76	-1.37	1.40	2.77